Near-ultraviolet micro-Raman study of diamond grown on GaN

M. Nazari,[1,a)] B. L. Hancock,[1] J. Anderson,[1] A. Savage,[1] E. L. Piner,[1,2] S. Graham,[3] F. Faili,[4] S. Oh,[4] D. Francis,[4] D. Twitchen,[4] and M. Holtz[1,2]
[1]*Materials Science, Engineering, and Commercialization, Texas State University, San Marcos, Texas 78666, USA*
[2]*Department of Physics, Texas State University, San Marcos, Texas 78666, USA*
[3]*Woodruff School of Mechanical Engineering, Georgia Institute of Technology, Atlanta, Georgia 30332-0405, USA*
[4]*Element Six Technologies, U.S. Corporation, Santa Clara, California 95054, USA*

(Received 15 December 2015; accepted 7 January 2016; published online 19 January 2016)

Ultraviolet (UV) micro-Raman measurements are reported of diamond grown on GaN using chemical vapor deposition. UV excitation permits simultaneous investigation of the diamond (D) and disordered carbon (DC) comprising the polycrystalline layer. From line scans of a cross-section along the diamond growth direction, the DC component of the diamond layer is found to be highest near the GaN-on-diamond interface and diminish with characteristic length scale of ~3.5 μm. Transmission electron microscopy (TEM) of the diamond near the interface confirms the presence of DC. Combined micro-Raman and TEM are used to develop an optical method for estimating the DC volume fraction. © *2016 AIP Publishing LLC*. [http://dx.doi.org/10.1063/1.4940200]

Gallium nitride is a technologically important semiconductor used in power electronics.[1] A major barrier limiting scaling and output power of transistors is self-heating which takes place in device active regions.[2,3] Notably, AlGaN/GaN heterojunction field-effect transistors (HFETs) operating at high power (7.8 W/mm) undergo large temperature rise (350 °C) in the active regions.[4] To achieve higher operating power in these devices, improvement in thermal management is critical. One way to mitigate self-heating in HFETs is to utilize substrates having higher thermal conductivity than traditional substrates Si and 6H-SiC. Diamond (D) films grown by chemical vapor deposition (CVD) are promising since they can be engineered to exhibit high thermal conductivity in the 800–2000 W/m · K range.[5–7]

The diamond CVD growth typically begins with a mix of highly disordered carbon (DC) and fine-grained polycrystalline diamond whose texture and size develop with increasing layer thickness. CVD diamond is generally grown in the graphitic region of the carbon equilibrium phase diagram thereby incorporating non-diamond phase (sp^2 and distorted sp^3). The nucleation layer may be nanoscale graphitic material as well as both graphitic and diamond-like amorphous carbon.[8] Here, we refer to the various non-diamond forms of carbon, including material comprising boundaries between polycrystals, as DC. As growth proceeds, polycrystalline diamond grains grow both laterally and vertically. Together with defects and grain boundaries in these films, the presence of DC/nucleation layer reduces the overall thermal conductivity of the diamond[5–7] with the most significant deleterious effects in the initial growth regions where the volume fraction of the DC (D), $f_{DC(D)} = V_{DC(D)}/(V_D + V_{DC})$, is greatest (least).

For diamond grown on a seeding layer on GaN, as described here, the quality of the initially formed diamond affects heat conduction both in the diamond layer and more importantly through the GaN-on-diamond (GaN/D) interface. Consequently, investigating CVD diamond film quality in the region closest to the GaN/D interface and as a function of distance (x) into the diamond film is crucial for optimizing direct growth on GaN for thermal management in HFETs.

Raman spectroscopy has been widely applied to carbon-based materials including CVD diamond, where film quality can be assessed based on the O(Γ)-symmetry Raman band at 1332 cm^{-1}. The DC component of diamond films is characterized by a broad peak from 1400 to 1700 cm^{-1}.[9–13] In visible Raman measurements, excitation of the π–π^* transitions of the sp^2-bonded carbon enhances its relative scattering intensity over diamond.[10] Unfortunately, the DC part of the Raman spectrum is generally difficult to discern due to the broad impurity-related photoluminescence (PL) background typical of CVD diamond.[10,14]

One approach for overcoming this limitation is to measure the Raman spectra using excitation wavelength of 363.8 nm which is beyond the impurity-related PL from the CVD diamond and excites σ-state transitions of both materials.[10] In this paper, we report near-ultraviolet (UV) micro-Raman spectroscopy to investigate diamond film morphology with particular interest in the GaN/D interface. Transmission electron microscopy (TEM) is used to estimate f_{DC} near the interface where the micro-Raman data show it to be highest.

We investigate materials grown to specifically integrate device-quality GaN with diamond. The GaN stack is grown on Si(111) substrate using metalorganic CVD.[15] Following this, a sacrificial carrier Si wafer is bonded to a SiN_x passivation layer first deposited on GaN. The growth substrate is then removed. A thin seeding layer is deposited on the GaN to prepare it for growth of the 100-μm thick microwave enhanced CVD diamond layer. Finally, the sacrificial silicon substrate is removed.[15] A 1-cm^2 coupon was diced from this wafer and a freshly cleaved cross-section was used for the scanning electron microscopy (SEM) and micro-Raman.

[a)]Author to whom correspondence should be addressed. Electronic mail: m_n79@txstate.edu.

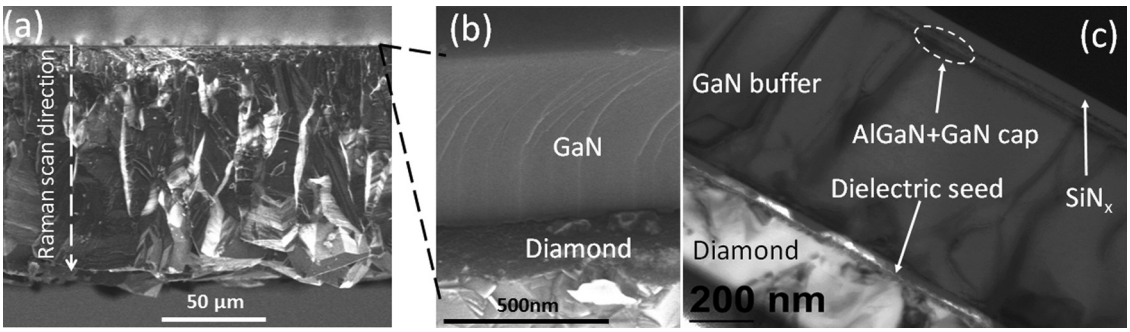

FIG. 1. SEM ((a) and (b)) and TEM (c) images of the diamond-on-GaN cross section. The arrow in (a) shows the direction of the micro-Raman line scan of diamond. (b) Close-up SEM of cleaved GaN. (c) TEM at the GaN/D interface. Dark regions in the diamond are associated with disordered carbon.

SEM and TEM measurements were used to investigate the morphology of the diamond and GaN. Figure 1(a) shows a SEM cross-section image of the cleaved surface. Due to its polycrystalline morphology, we do not obtain a smooth cross-section. In contrast, the GaN layer is much more crystallographically oriented as shown in the detailed SEM image of the GaN/D interface region in Fig. 1(b).

Figure 2 summarizes the Raman data. Fig. 2(a) inset shows the micro-Raman spectrum of the diamond excited using 514.5 nm and 363.8 nm laser light. Measured power at the sample is 200 μW, with spot size of $\sim$3 μm in diameter and acquisition time from 2 to 3 min. The sharp O(Γ) diamond phonon at 1332 cm^{-1} is clearly observed. In addition, the strong impurity-related PL background is also seen in the visible spectrum. Figure 2(a) shows UV micro-Raman spectra obtained at different positions within the diamond layer relative to the GaN/D interface ($x = 0$). The DC intensity diminishes with increasing x. Figure 2(b) shows the UV micro-Raman spectra of GaN/D taken in plan view from the diamond side of the sample and from the cross-section surface (with laser light focused at the GaN/D interface). Because diamond is transparent to the 363.8-nm excitation, which is near resonance with the GaN direct band-gap transition, the observed Raman intensity is high for both materials. Selection rules differ for backscattering along and perpendicular to the GaN c axis. In plan view, the E_2^2 and A$_1$(LO) phonons are located at 566.8 and 735.8 cm^{-1}, respectively. Due to the resonance conditions, strong second-order A$_1$(LO) scattering is also seen. For backscattering perpendicular to the c-axis, we observe allowed scattering from the E$_1$(TO), E_2^2, and quasi-longitudinal-optic[16] q-E$_1$(LO) phonons at respective energies of 558.7, 566.8, and 738.4 cm^{-1} as well as strong second-order q-E$_1$(LO) at 1476.2 cm^{-1}.

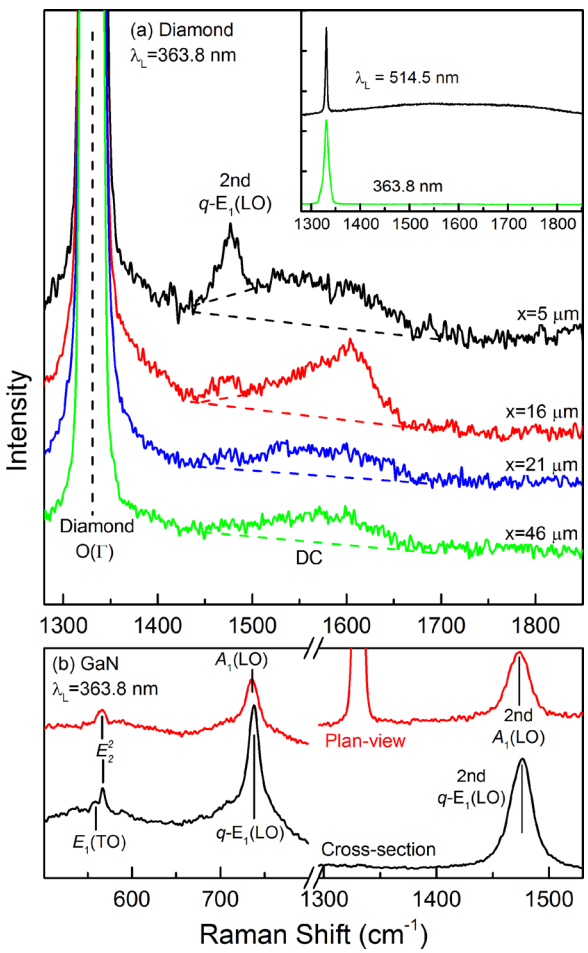

FIG. 2. (a) Near-UV micro-Raman spectra of diamond 1332 cm^{-1} and disordered carbon range of 1400–1700 cm^{-1} at select distances from GaN/D interface. The peak at 1476 cm^{-1} in (a) is from GaN. The inset shows micro-Raman spectra of diamond-on-GaN sample using 514.5 and 363.8 nm excitation with no background subtraction. (b) Plan view and cross-section micro-Raman spectra of GaN.

For the micro-Raman line scans, the cleaved sample was vertically affixed to an automated translational stage with 0.2-μm minimum step size. The GaN/D interface was located based on the position-dependent amplitude of the GaN and diamond phonons (not shown). By moving in the direction of the arrow shown in Fig. 1(a), the Raman amplitude of the GaN bands decreases as the diamond peak rises and subsequently levels off. The interface is identified as the position where the two normalized dependences cross.

In addition to the intense O(Γ) diamond peak shown in Fig. 2(a), we observe the broad and weak DC features at 1400–1700 cm^{-1}. The intensity of this region decreases with distance from GaN/D interface. The peak near 1476 cm^{-1} in the $x = 5$ μm spectrum is the second-order q-E$_1$(LO) phonon of GaN. Remnants of this feature are detected at this distance from the GaN/D interface, possibly due to refraction of the laser light at the non-planar diamond surface into the nearby GaN.

Figure 3(a) summarizes the O(Γ) diamond peak position as a function of distance from the GaN/D interface from line scans at two different locations of the cross-section. Due to the polycrystalline nature of the diamond film, the D peak

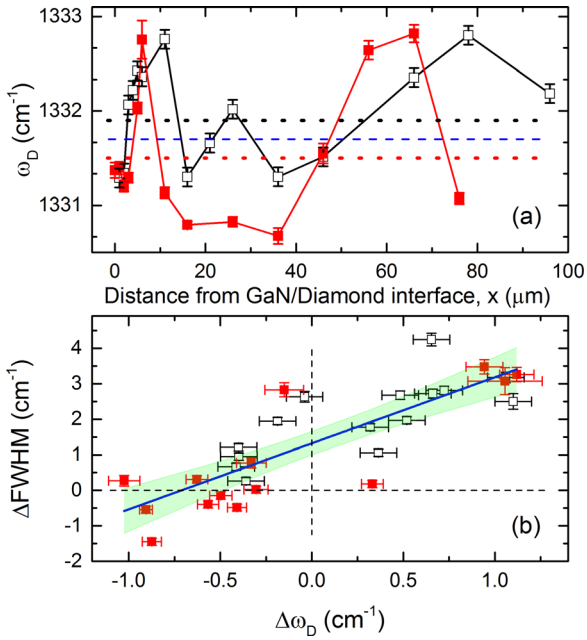

FIG. 3. (a) Diamond peak position from line scans obtained at two different locations of the GaN/D cross-section. Horizontal dotted lines are average values from scans 1 and 2. Dashed line shows reference diamond at 1331.7 cm^{-1}. (b) Relative FWHM as a function of relative peak position from reference diamond. A linear fit is shown to the combined data sets and shaded area corresponds to 95% confidence interval band.

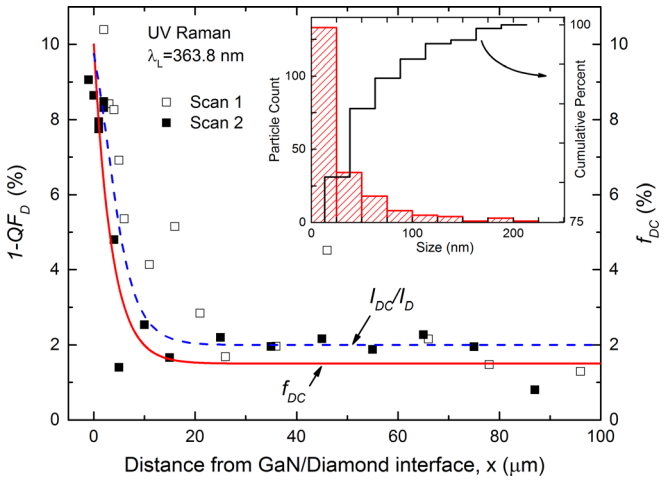

FIG. 4. Quantity $1-QF_D$ based on diamond and DC integrated Raman intensities as a function of distance from the interface from two line scans. The dependence is used to model $f_{DC}(x)$ with $x=0$ value of 10% estimated from TEM analysis. Dashed curve shows relative intensities and solid curve is $f_{DC}(x)$, right-hand axis. The decreasing trend has characteristic length scale of $\sim$3.5 μm reaching $f_{DC}\sim 2\%$ at 20 μm. Inset is a histogram of TEM image analysis of DC average particle size.

varies with average values at $1331.9 \pm 0.1\,\mathrm{cm}^{-1}$ (scan 1) and $1331.5 \pm 0.1\,\mathrm{cm}^{-1}$ (scan 2). This is compared to the value for a reference diamond at $1331.7\,\mathrm{cm}^{-1}$ (dashed blue line in the inset) measured immediately prior to the start of each scan. Variation along the scan direction may be attributed to local stresses within the diamond polycrystals.[17] Variations are also observed in the line width (not shown) with overall dependence reminiscent of what is seen in the peak position data. In Fig. 3(b), we summarize line width data versus measured peak position, each relative to reference diamond. A linear fit is shown along with 95% confidence interval bands. Evidently, the relative peak position and width are correlated, an effect which has been previously attributed to local stress gradients in polycrystalline diamond as well as variations in defect density.[18]

As mentioned before, the broad feature labeled DC in the Raman spectra of Fig. 2(a) is related to different forms of carbon, other than the desired diamond, and therefore may be used as a further measure of structural homogeneity. A useful quantity for this is the Raman quality factor[19] based on the integrated Raman intensities of the diamond peak and DC band, defined $QF_D = \left[\frac{I_D}{I_D+I_{DC}}\right]$. In this regard, the quantity $1-QF_D = \left[\frac{I_{DC}}{I_D+I_{DC}}\right] \approx \left[\frac{I_{DC}}{I_D}\right]$ is a measure of the DC presence in the layer. Figure 4 summarizes the dependence of the $\left[\frac{I_{DC}}{I_D+I_{DC}}\right]$ along the diamond growth direction from the GaN/D interface from the same two line scans summarized in Fig. 3. Overall consistency is observed although it is clear that lateral variations in morphology are also present.

The data in Fig. 4 confirm that diamond growth begins with material that has higher DC content and this fraction diminishes with diamond thickness to result in diamond with little DC. Intensities in spontaneous Raman scattering are proportional to volume probed. For the mixed DC/D medium investigated here, the relative intensities are an indication of the relative volumes V_{DC}/V_D probed. Because intensities are also a function of the material- and wavelength-dependent Raman tensor and optical properties, the ratio plotted in Fig. 4 does not correspond to the relative volume and may only be regarded as the trend in this quantity.

To obtain an independent measure of the DC volume fraction f_{DC}, cross-sections were prepared for TEM imaging using a SEM-based focused ion beam (FIB) "lift-out" technique. Imaging of the final prepared cross-section was carried out in a TEM microscope (JEOL JEM1200) in bright field mode. Figure 1(c) shows a representative TEM image of the GaN/D cross-section with dielectric seed, GaN buffer, AlGaN barrier plus GaN cap (not resolved), and SiN_x dielectric passivation layer. Darker regions observed in the diamond layer of the TEM image are attributed to growth imperfections where the DC is formed near the diamond seed and at grain boundaries,[20–22] and to a local high density of grain boundaries. Electron energy loss spectroscopy confirms the presence of sp^2-coordinated carbon but does not provide us with a material volume fraction.

A region near the GaN/D interface, $\sim$5 μm in length and 300 nm thick, was analyzed based on TEM to estimate f_{DC}. This region is of interest because it is closest to the interface where the diamond growth initiates and where the DC presence is observed to be highest. Clearly observed in the TEM images are structural imperfections in both the diamond and the GaN layers. Due to the different TEM contrasts between the diamond and DC, the TEM may be used to estimate volume fractions of the two materials.[20–22] Dark regions in Fig. 1(c) are associated with structural disorder—grain boundaries, defects, and regions where the onset of carbon deposition during diamond CVD—we denote as DC.

Based on the 256-level black/white contrast, we establish the black threshold based on regions of the image which

were clearly dark in TEM data, and which we attribute to DC. This value varies slightly between the different images due to subtle differences in acquisition conditions. Analysis of the number of pixels binned as DC to the total number in the image is used to estimate V_{DC}/V_D and the corresponding f_{DC}. Our analysis results in $f_{DC} \sim 8\%$ to 12%, depending on the threshold, for the 300-nm thick region studied in the GaN/D interface range. We use a nominal value of 10% for this volume fraction. This result is close to what has been previously reported for CVD diamond grown on Si,[11] and Si and 6H-SiC[13] substrates. However, it is important to note that our method includes the presence of grain boundaries which overestimates f_{DC}. The image processing also reveals the size of contiguous DC regions. The inset of Fig. 4 shows a histogram illustrating the size distribution. Approximately, 80% of the DC regions are $\lesssim 25$ nm across in the TEM image.

The f_{DC} value obtained from the TEM data may now be used to scale the dependence in Fig. 4 to obtain an estimate of the DC presence based on the Raman measurements. However, simply assigning, the initial value in the relative intensities to the $f_{DC} \sim 10\%$ is not sufficient. This is because the TEM data sampled $\sim$300 nm thick GaN/D interface regime, while our micro-Raman measurements probe a region $\sim 3\,\mu$m in diameter and therefore represent an average over this region. To account for the larger region sampled in the micro-Raman measurement, the intensity is treated as a convolution of the position-dependent volume fraction and the laser illumination

$$\frac{I_{DC}}{I_D}(x) \approx A \frac{\int_0^t f_{DC}(x')\Phi(x-x')dx'}{\int_0^t \Phi(x-x')dx'}, \tag{1}$$

where x is the central position of the laser spot along the growth direction, $x = 0$ is the GaN/D interface, and t is the diamond thickness. We discuss proportionality factor A below. The laser illumination $\Phi(x)$ is assumed to have a Gaussian shape with root-mean squared width $3/\sqrt{2} = 2.1\,\mu$m. By varying x from 0 to t and integrating over x' at each position x, we average the function $f_{DC}(x)$ over the laser spot size.

Based on the dependence observed in Fig. 4 for the intensity ratio, we suppose a simple dependence for the DC volume fraction

$$f_{DC}(x) = (f_0 - f_t)e^{-x/d} + f_t, \tag{2}$$

with f_0 (f_t) being the DC volume fraction at (far from) the GaN/D interface. Quantity d is a distance over which f_{DC} diminishes and is expected to depend on several factors related to the growth method and conditions. Using $f_0 = 10\%$ from TEM in Eq. (2), we fit the Raman intensity data in Fig. 4 using Eq. (1) to obtain parameters $f_t = 1.5\%$ and $d = 3.5 \pm 0.5\,\mu$m. The dashed curve shows the resulting dependence from Eq. (1). The solid curve in Fig. 4 is the corresponding function $f_{DC}(x)$ with scale on the right-hand axis. The model proposed for Eq. (2) seems reasonable and fits the data well. The two individual data sets in Fig. 4 give values for d of 5.5 ± 0.5 and $2.7 \pm 0.2\,\mu$m for scans 1 and 2, respectively, illustrating a lateral dependence in diamond growth properties.

The importance of this result is that it may now be used as a stand-alone Raman method for estimating f_{DC} without the need of TEM analysis. However, it is important to reproduce the conditions of our measurement for the approach to be valid, in particular, the excitation wavelength used. This is necessary for obviating the background PL but also due to the wavelength dependence of the Raman tensors and optical properties of DC and diamond. From our approach, applied here to the data in Fig. 4, the proportionality factor A in Eq. (1) may be estimated. We obtain from this analysis a value of $A = 1.3 \pm 0.1$. This factor is related to the relative Raman cross section of DC and diamond material for UV (363.8 nm) light. Previous investigators have also considered the relative intensities of D and DC. Taking into account that the DC peak is 75 times more sensitive to visible (514.5 nm) excitation than diamond, Silveira *et al.* used integrated Raman intensities to estimate diamond percentage in films grown by plasma-assisted CVD. Values obtained for diamond percentage were reported in 89%–96% range.[11] Similarly Sails *et al.* and Das *et al.* used relative Raman cross section of 233 at 514.5 nm to obtain f_D ranging from 85% to nearly 100%.[13,19] Deep UV (244 nm) Raman measurements have also been applied to estimate f_D.[10] At this wavelength, the relative cross section for D and DC peaks is taken to be $\sim$1 although volume fractions are not specifically investigated. The significant change in sensitivity to DC is attributed to tuning the excitation away from the π–π^* transitions in the visible with enhanced sp^2 sensitivity, and toward the σ-state transitions of both sp^2 and sp^3 in the UV. Evidently, the 363.8 nm Raman excitation has a relative sensitivity of DC to D of approximately $A = 1.3$.

In summary, we studied diamond grown on GaN using UV micro-Raman spectroscopy. Raman intensity along with TEM image analysis is used to estimate non-diamond carbon volume fraction in the film as a function of distance from GaN/D interface. Early stages of growth result in $\sim$10% DC. This value decreases exponentially with a characteristic length scale $d \sim 3.5\,\mu$m and is negligible by $20\,\mu$m after which f_{DC} remains constant. The analysis also gives relative Raman cross section of DC and diamond material for 363.8-nm light to be 1.3. From the TEM analysis, the majority (>80%) of the DC regions near the GaN/D interface have size $\lesssim$25 nm. The approach reported here allows determining f_{DC} based solely on micro-Raman measurements, while the evaluation of typical DC particle size requires TEM studies. A limitation to the micro-Raman approach is laser spot size which produces an average of the relative intensities and f_{DC}. Uncertainty in I_{DC} is attributed to noise in the spectrum, which is <10%. The impact of this on the f_{DC} estimate from Raman measurements is $\sim$1%, which is small compared to position-dependent variations seen in Fig. 4. The significance of applying these approaches is to aid in the development of CVD diamond growth and to provide input for modeling approaches to describe thermal properties of the material for use in designing heat spreading layers.

Texas State University and Georgia Tech acknowledge DARPA for partial support of this work.

[1]E. A. Jones, F. Wang, and B. Ozpineci, in *IEEE Workshop on Wide Bandgap Power Devices and Applications (WiPDA)* (2014), pp. 24–29.
[2]J. Kuzmik, M. Tapajna, L. Valik, M. Molnar, D. Donoval, C. Fleury, D. Pogany, G. Strasser, O. Hilt, F. Brunner, and J. Wurfl, IEEE Trans. Electron Devices **61**, 3429 (2014).
[3]J. T. Asubar, Z. Yatabe, and T. Hashizume, Appl. Phys. Lett. **105**, 053510 (2014).
[4]M. Nazari, B. L. Hancock, E. L. Piner, and M. W. Holtz, IEEE Trans. Electron Devices **62**, 1467 (2015).
[5]R. H. Zhu, J. Y. Miao, J. L. Liu, L. X. Chen, J. C. Guo, C. Y. Hua, T. Ding, H. K. Lian, and C. M. Li, Diamond Relat. Mater. **50**, 55 (2014).
[6]A. V. Sukhadolau, E. V. Ivakin, V. G. Ralchenko, A. V. Khomich, A. V. Vlasov, and A. F. Popovich, Diamond Relat. Mater. **14**, 589 (2005).
[7]D. J. Twitchen, C. S. J. Pickles, S. E. Coe, R. S. Sussmann, and C. E. Hall, Diamond Relat. Mater. **10**, 731 (2001).
[8]P. K. Chu and L. Li, Mater. Chem. Phys. **96**, 253 (2006).
[9]R. E. Shroder, R. J. Nemanich, and J. T. Glass, Phys. Rev. B **41**, 3738 (1990).
[10]S. M. Huang, Z. Sun, Y. F. Lu, and M. H. Hong, Surf. Coat. Technol. **151–152**, 263 (2002).
[11]M. Silveira, M. Becucci, E. Castellucci, F. P. Mattiot, V. Barbarossa, R. Tomaciello, and F. Galluzzi, Diamond Relat. Mater. **2**, 1257 (1993).
[12]M. Nishitani-Gamo, T. Ando, K. Watanabe, M. Sekita, P. A. Dennig, K. Yamamoto, and Y. Sato, Diamond Relat. Mater. **6**, 1036 (1997).
[13]D. Das, V. Jayaseelan, R. Ramamurti, R. S. Kukreja, L. Guo, and R. N. Singh, Diamond Relat. Mater. **15**, 1336 (2006).
[14]B. Marchon, J. Gui, K. Grannen, G. C. Rauch, and J. W. Ager III, IEEE Trans. Magn. **33**, 3148 (1997).
[15]F. Ejeckam, D. Francis, F. Faili, D. Twitchen, B. Bolliger, D. Babic, and J. Felbinger, in *Lester Eastern Conference on High Performance Devices (LEC)* (2014), p. 1.
[16]L. Bergman, M. Dutta, C. Balkas, R. F. Davis, J. A. Christman, D. Alexson, and R. J. Nemanich, J. Appl. Phys. **85**, 3535 (1999).
[17]S. Prawer and R. J. Nemanich, Philos. Trans. R. Soc., A **362**, 2537 (2004).
[18]J. W. Ager, D. K. Veirs, and G. M. Rosenblatt, Phys. Rev. B **43**, 6491 (1991).
[19]S. R. Sails, D. J. Gardiner, M. Bowden, J. Savage, and D. Rodway, Diamond Relat. Mater. **5**, 589 (1996).
[20]C. B. Lioutas, N. Vouroutzis, S. Logothetidis, and H. Lefakis, Thin Solid Films **319**, 144 (1998).
[21]T. Harigai, Y. Yasuoka, N. Nitta, H. Furuta, and A. Hatta, Diamond Relat. Mater. **38**, 36 (2013).
[22]V. Ralchenko, L. Nistor, E. Pleuler, A. Khomich, I. Vlasov, and R. Khmelnitskii, Diamond Relat. Mater. **12**, 1964 (2003).